



Contents lists available at ScienceDirect

## Journal of Colloid and Interface Science

journal homepage: [www.elsevier.com/locate/jcis](http://www.elsevier.com/locate/jcis)

## Regular Article

## Enabling Marangoni flow at air-liquid interfaces through deposition of aerosolized lipid dispersions



Amy Z. Stetten<sup>a</sup>, Grace Moraca<sup>a</sup>, Timothy E. Corcoran<sup>b</sup>, Stephanie Tristram-Nagle<sup>a</sup>, Stephen Garoff<sup>a,\*</sup>, Todd M. Przybycien<sup>c,d</sup>, Robert D. Tilton<sup>c,d</sup>

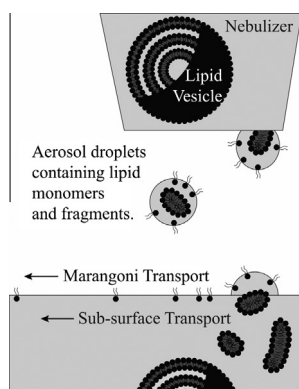
<sup>a</sup>Center for Complex Fluids Engineering, Department of Physics, Carnegie Mellon University, Pittsburgh, PA 15213, USA

<sup>b</sup>Center for Complex Fluids Engineering, Department of Medicine, University of Pittsburgh, Pittsburgh, PA 15260, USA

<sup>c</sup>Center for Complex Fluids Engineering, Department of Biomedical Engineering, Carnegie Mellon University, Pittsburgh, PA 15213, USA

<sup>d</sup>Center for Complex Fluids Engineering, Department of Chemical Engineering, Carnegie Mellon University, Pittsburgh, PA 15213, USA

## GRAPHICAL ABSTRACT



## ARTICLE INFO

## Article history:

Received 7 July 2016

Revised 29 August 2016

Accepted 30 August 2016

Available online 31 August 2016

## Keywords:

Marangoni flow  
Surface transport  
Surfactant  
Phospholipid  
Aerosol

## ABSTRACT

It has long been known that deposited drops of surfactant solution induce Marangoni flows at air-liquid interfaces. These surfactant drops create a surface tension gradient, which causes an outward flow at the fluid interface. We show that aqueous phospholipid dispersions may be used for this same purpose. In aqueous dispersions, phospholipids aggregate into vesicles that are not surface-active; therefore, drops of these dispersions do not initiate Marangoni flow. However, aerosolization of these dispersions disrupts the vesicles, allowing access to the surface-active monomers within. These lipid monomers do have the ability to induce Marangoni flow. We hypothesize that monomers released from broken vesicles adsorb on the surfaces of individual aerosol droplets and then create localized surface tension reduction upon droplet deposition. Deposition of lipid monomers via aerosolization produces surface tensions as low as 1 mN/m on water. In addition, aerosolized lipid deposition also drives Marangoni flow on entangled polymer solution subphases with low initial surface tensions ( $\sim 34$  mN/m). The fact that aerosolization of phospholipids naturally found within pulmonary surfactant can drive Marangoni flows on low surface tension liquids suggests that aerosolized lipids may be used to promote uniform pulmonary drug delivery without the need for exogenous spreading agents.

© 2016 Elsevier Inc. All rights reserved.

\* Corresponding author.

E-mail addresses: [astetten@andrew.cmu.edu](mailto:astetten@andrew.cmu.edu) (A.Z. Stetten), [gmoraca1901@gmail.com](mailto:gmoraca1901@gmail.com) (G. Moraca), [corcoranTE@upmc.edu](mailto:corcoranTE@upmc.edu) (T.E. Corcoran), [stn@cmu.edu](mailto:stn@cmu.edu) (S. Tristram-Nagle), [sg2e@andrew.cmu.edu](mailto:sg2e@andrew.cmu.edu) (S. Garoff), [todd@andrew.cmu.edu](mailto:todd@andrew.cmu.edu) (T.M. Przybycien), [tilton@andrew.cmu.edu](mailto:tilton@andrew.cmu.edu) (R.D. Tilton).

## 1. Introduction

For years, researchers have studied the ability of Marangoni flows to induce surface transport. Marangoni flows most commonly occur when localized deposition of a surface-tension-lowering agent such as a surfactant causes a surface tension gradient to develop (for examples, see references [1–4]). This gradient induces a convective Marangoni flow outward from the region of deposition. Induced Marangoni flow has potential use in improving drug delivery in patients with obstructive pulmonary conditions such as cystic fibrosis lung disease, where accumulation of dehydrated mucus alters airway aerodynamics and subsequent patterns of aerosol deposition in the lung (for examples, see references [5–7]).

Previous work from our group has shown that a variety of surfactants cause surface tension reduction and Marangoni flow when delivered to air-liquid interfaces as long as the surface tension of the solution is lower than that of the subphase. Various soluble surfactants such as sodium dodecylsulfate (SDS) anionic surfactant, Capstone FS-3100 nonionic fluorosurfactant, hexadecyltrimethylammonium bromide cationic surfactant, and Tyloxapol nonionic surfactant have been shown to be good spreaders on various model subphases [8–11]. Due to their potential use in pulmonary drug delivery applications, we have examined the ability of phospholipids, natural components of pulmonary surfactant, to induce Marangoni flow.

Phospholipids have never been studied as spreading agents, but they are already being used in the lung as components of drug formulations treating infant respiratory distress syndrome (IRDS). In this context their role is surface tension reduction in the pulmonary respiratory zone. Most currently marketed surfactant replacement therapies (SRTs) used in IRDS treatment are multi-component dispersions of purified lung surfactant from animals. These contain lipid as well as peptide components. Previous work from our group has shown that these multicomponent SRTs can do more than just lower surface tension; when aerosolized, they can initiate Marangoni flow [12]. In this paper we show that even single-component phospholipid vesicle dispersions induce Marangoni flow, provided that they are aerosolized en route to deposition. Thus, aerosolization may enable phospholipids to serve as spreading agents without the need for other excipients.

There has been a significant amount of previous work to study the surface activity of phospholipids such as dipalmitoylphosphatidylcholine (DPPC), comprising investigations of lipid monolayers deposited out of organic solution and investigations of aqueous dispersions of DPPC. The former are the familiar Langmuir trough studies of lipid monolayer surface pressure–molecular area behavior. The latter involve preparing lipid vesicle dispersions and monitoring their surface tensions as some vesicles break open and release surface-active lipid molecules. Both types of investigations focus on the ability of phospholipids (or phospholipids in combination with other components such as lung peptides) to lower surface tension; they do not directly probe phospholipids' ability to initiate Marangoni flow on a liquid surface (for examples, see [13–18]).

Franses and his coworkers have extensively studied the surface-active properties of DPPC. In their work, they see that freshly prepared aqueous dispersions of DPPC have surface tensions near that of water, and then decrease in surface tension at rates depending on lipid processing. In the absence of surface compression/expansion cycles, the long-time surface tensions of these dispersions ranged from 63 mN/m achieved over about an hour and a half for larger vesicles down to 48 mN/m achieved over an hour for the smallest prepared vesicles in their experiments [13–15,19].

The vesicles contained in phospholipid dispersions are not surface active at the air/water interface in their intact form. The

hydrophobic tails are sequestered within bilayers, and the head groups lack an attraction to the air/water interface. Furthermore, the vesicles are stable and exist in equilibrium with an extremely low concentration of free lipid monomer (the dominant surface tension lowering species) in solution, on the order of  $10^{-8}$  M [20]. At these small concentrations of free monomers, the surface-active material to be found in these dispersions is insufficient to rapidly and locally lower the surface tension, a condition necessary to induce Marangoni flow. The mechanism behind any significant surface tension reduction of these dispersions is understood as two processes in series, one diffusional and one kinetic. To create an adsorbed layer vesicles must first diffuse to the surface, and then those at the surface must break open to reveal surface-active lipid monomers. Over short times and for low concentrations of lipid, this system is regulated by diffusion and no measurable surface pressure is created. Over longer times and for higher lipid concentrations, a surface layer is created that lowers the surface tension of the dispersion. There is evidence that the resulting surface layer may not be simply a monolayer; it is most likely made up of multilayer mesophases [13,14,16].

Although all of the DPPC dispersions that were studied in the aforementioned references did, eventually, show lower surface tensions than that of water, the authors did not attempt to use the dispersions as transport agents to initiate Marangoni flow across a liquid surface. Therefore, we prepared similar dispersions and deposited them as microliter drops onto a water subphase. These dispersions did have lower surface tensions than water, however they showed no evidence of induced Marangoni transport. Typically if one deposits a drop of fluid onto a subphase that has higher surface tension than that of the drop, the gradient in surface tension will induce flow towards the higher surface tension region. However, we are depositing very small volume (microliter) drops onto a much larger volume (20 mL) subphase. These small deposited volumes produce dilute dispersions upon mixing into the subphase. According to Launois-Surpas and coworkers, dilute dispersions have slow rates of surface-induced vesicle break-up, and thus the process of surface tension reduction is diffusion-limited and negligible surface pressures will be created [16].

In this paper, we show that aerosolization is one method by which we may induce aqueous phospholipid dispersions to create the surface tension gradient required for Marangoni spreading. Prior work has shown that aerosolization can break liposomes down into smaller aggregates [21,22] and can break open the aggregates contained in SRT formulations [23]. We postulate that aerosolization can do the same to the stable multilamellar vesicles of pure DPPC and dimyristoylphosphatidylcholine (DMPC) dispersions; it can allow surface-active monomer to be released, perhaps stored by adsorption on the surfaces of individual microscopic aerosol droplets, and transferred onto a fluid subphase after droplet deposition. This will result in the creation of a lipid monolayer created by fusion of the lipid layers from the many depositing aerosol droplets, which will locally lower the surface tension of the subphase. When aerosol deposition is confined to a limited region of the subphase, the surface tension gradient induced by this local surface tension reduction will induce Marangoni transport across the surface.

## 2. Materials and methods

### 2.1. Materials

DMPC and DPPC were purchased from Avanti Polar Lipids in the lyophilized form (>99% purity) and were used without further purification. DMPC was chosen for our primary experiments

because it is very similar to DPPC, the most abundant lipid in natural pulmonary surfactant, but has a main phase transition temperature for bulk samples ( $T_M$ ) of 24 °C [24], whereas DPPC's is 41.4 °C [25]. All experiments were performed between 24 and 26 °C.

Primary experiments were conducted using dispersions of multilamellar lipid vesicles (MLVs) prepared using a standard temperature-cycling process [26]. We prepared a 20 mL vial of 10 mg/mL DMPC or DPPC in deionized (DI) water. The deionized water was purified using a Millipore, Milli-Q Academic unit and had a resistivity of 18 M $\Omega$  cm and a surface tension of  $72.7 \pm 0.7$  mN/m; the quoted uncertainty here and elsewhere in this article is the standard error of the mean. The lyophilized lipids and water were first mixed for 30 s using a vortex mixer (Fisher Scientific Analog Vortex Mixer, CAT# 02215365). The dispersion was then warmed  $\sim 20$  °C above  $T_M$ , into its fluid phase, for 10 min, mixed on the vortex mixer for 30 s, and then chilled  $\sim 20$  °C below  $T_M$  for an additional 10 min. This process was repeated three times in order to achieve a dispersion of approximately 10  $\mu$ m diameter MLVs [27].

Secondary experiments were conducted using dispersions of small unilamellar vesicles (SUVs) prepared using ultrasonication. Again, we prepared a 20 mL vial of 10 mg/mL phospholipid in DI water. The lyophilized lipids and water were then sonicated at least 20 °C above  $T_M$  using a probe ultrasonicator (Branson Sonifier Cell Disruptor 185, Emerson Electric Co.) in 3 min bursts, allowing the dispersion to cool for 5 min in between bursts. This process was continued until the dispersions were optically clear yielding approximately 250–450 Å SUVs [28,29].

Three subphases were used in this work: DI water, aqueous porcine gastric mucin solutions (PGM), and aqueous poly(acrylamide) solutions (PA). Porcine gastric mucin (PGM; Type II, bound sialic acid  $\sim 1\%$  CAS# 84082-64-4) was purchased from Sigma Aldrich. The PGM was stored between 2° and 8 °C while not in use and was rehydrated with DI water. A 5% w/w solution of PGM was prepared in DI water and stirred magnetically for  $\sim 14$  h, at which point the solution was visually homogeneous. The 5% w/w concentration is above the entanglement concentration of PGM in water [11,30]. The prepared PGM solutions were stored between 2° and 8 °C and used within 4–5 days of preparation. The surface tension of the 5% w/w PGM solution was  $38.3 \pm 3.5$  mN/m, and typically decreased by 2–3 mN/m over 5 min after pouring a fresh sample.

Poly(acrylamide) of molecular mass 5–6 MDa (CAS# 9003-05-08) was purchased in powder form from Polysciences (Warrington, PA) and used as received. Aqueous solutions of 1% w/w PA were prepared in DI water by adding the PA powder in increments of 2 g every 2–3 days in a 3/4 full 1 L bottle under nitrogen with continuous gentle mixing on a gyratory shaker (New Brunswick Scientific, Edison, NJ, model G79, speed “4”). After adding the final 2 g of powder, water was added to bring the total volume up to 1 L, and stirring continued for 2–3 more days or until the solution was homogeneous, whichever took longer. PA solution concentrations were above the previously reported 0.45% w/w entanglement concentration [10]. The surface tension of the PA solution after pouring a fresh sample was  $70.8 \pm 0.5$  mN/m, which typically decreased by  $\sim 1$ –2 mN/m over 5 min.

## 2.2. Methods

Most aerosolization experiments were performed with an AeroNeb Solo micropump nebulizer (Aerogen, Galway, Ireland) with an Aerogen Pro-X controller. Each nebulizer consists of a fluid chamber, at the bottom of which is a 5 mm wide mesh plate containing approximately 1000 tapered,  $4.8 \pm 0.3$   $\mu$ m holes. When this mesh is vibrated at  $1.2 \times 10^5$  cycles per second, the holes act as micro

pumps, each pumping out uniform droplets of dispersion. Aerosol droplet size was measured by laser diffraction using a Malvern Mastersizer. For aerosolized DMPC dispersions, the volume median droplet diameter was  $5.7 \pm 0.1$   $\mu$ m (with volume weighted 10th and 90th percentile values of  $2.5 \pm 0.1$   $\mu$ m and  $11.1 \pm 0.4$   $\mu$ m). As a reference, the average droplet diameter for 0.9% saline solution was  $4.3 \pm 0.1$   $\mu$ m (with volume weighted 10th and 90th percentile values of  $2.0 \pm 0.1$   $\mu$ m and  $8.4 \pm 0.3$   $\mu$ m).

In a second set of experiments designed to determine whether the mechanism of aerosol generation would affect the ability of lipid dispersions to drive Marangoni flows, we used an AeroEclipse® II Breath Actuated Nebulizer purchased from the Monaghan Medical Corporation in Plattsburgh, NY. In this nebulizer, fluid is drawn up through narrow tubing, driven by a dry nitrogen flow of between 3 and 8 L per minute, forming a jet that breaks up into small aerosol droplets due to capillary instabilities.

Both of these medical nebulizers were designed to deliver a consistent dose of medication when the full reservoir is emptied. The rate of nebulization can vary during the emptying of the reservoir, as discussed below. In addition, the total time to empty the reservoir can vary from nebulizer to nebulizer and trial to trial. Despite this variability in nebulization rates, consistent experimental trends yielded robust conclusions.

We built an experimental trough setup designed to permit simultaneous measurement of surface tension and observation of Marangoni flow outside of the region of aerosol deposition (see Fig. 1). The setup consisted of a poly(vinyl chloride) trough 2 cm wide by 2 cm deep by 20 cm long. This trough was filled with 20 mL of deionized water, or other subphases as specified, giving a depth of 0.5 cm. At this depth, the gravitational parameter  $G > 3$ ;  $G = \rho g H^2 / S$  where  $\rho$  is the subphase density, 1000 kg/m<sup>3</sup>,  $g$  is acceleration due to gravity,  $H$  is subphase depth, and  $S$  is the surface tension of the clean surface minus that of the deposited dispersion, which is at most 72 mN/m [2]. When this parameter is greater than 0.5, as it is in our case, recirculation beneath the advancing capillary ridge can occur in the subphase and dewetting of the underlying solid surface should not, and does not, occur [2].

This water-filled trough extended through a small opening half way into a clear acrylic box. The acrylic box housed the nebulizer and served to contain the depositing aerosol. In this way, direct aerosol deposition was confined to the half of the trough within the acrylic box. Little aerosol escaped the box as indicated by laser scattering near the exit. Within 20 s of turning on the nebulizer (for a  $\sim 10$  min experiment), the containment box reaches 90% relative humidity. Within 30 s, the relative humidity reaches 95% and continues to increase slowly with time. We, therefore, believe that drying of the aerosol is not a significant effect. The surface tension was monitored with a Wilhelmy pin apparatus (Nima Technology Limited, Coventry, England). A platinum Wilhelmy pin was used for all experiments. Fluid flow at the surface was observed using a small polystyrene indicator bead,  $\sim 1$  mm in diameter, placed on the fluid surface just outside of the acrylic box and observed with a Nikon 3600 digital camera. Images were analyzed using NIS-Elements Advanced Research software (Nikon Instruments Inc, Melville, NY) to track the particle trajectory. The indicator bead centered itself in the trough due to capillary forces, thus only the position along the length of the trough varied with time.

DMPC surface pressure/area isotherms on water were measured in a 14 cm glass petri dish using the Wilhelmy pin apparatus. The phospholipid was dissolved in chloroform and deposited dropwise onto a water surface using a glass syringe. The chloroform was allowed to evaporate and the surface tension was allowed to equilibrate after each drop was deposited. The area per molecule was calculated using the concentration of the solution, the volume

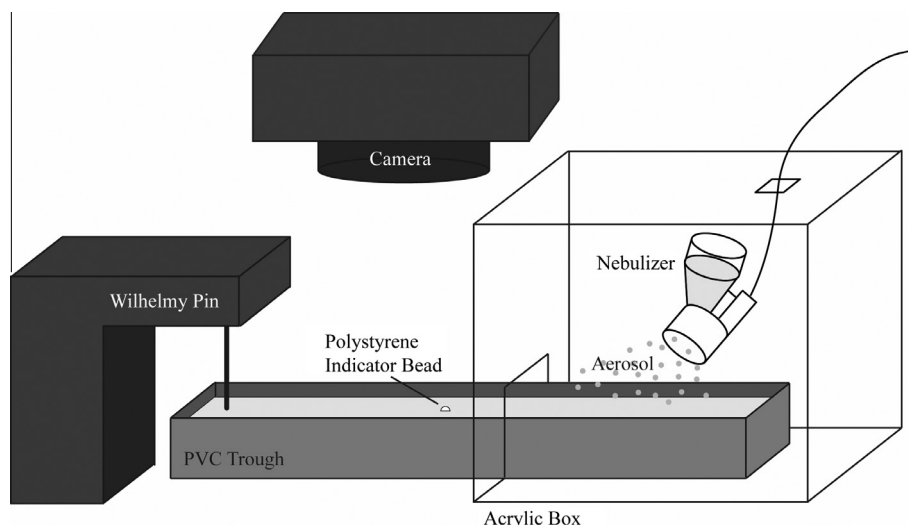


**Fig. 1.** Diagram of trough setup. Dimensions of the trough are 20 cm long by 2 cm wide by 2 cm deep. The aerosol deposition is perpendicular to the long axis of the trough at a declination of approximately 45°.

of the drops deposited, and the size of the petri dish. Our isotherm, shown in the supplemental information, is in good agreement with literature isotherms for DMPC at room temperature (see, for example, references [31–35]). In the literature for monolayers at room temperature, the area per molecule at which the isotherms lift off (when a detectable non-zero surface pressure is achieved) is reported between 90 and 130 Å<sup>2</sup> per molecule. The area per molecule at monolayer collapse is reported between 45 and 60 Å<sup>2</sup> per molecule. These lift-off and collapse areas match well with our isotherm. The actual surface pressure at collapse, which is the result of kinetic processes, varies depending on the method and experimental details used to create and compress the monolayer. References for DMPC isotherms created using a Langmuir trough give collapse pressures between 37 and 71 mN/m [31–35]. This wide variability is likely due to differences in the experimental conditions used to collect the data. More recent trough studies tend to give higher collapse pressures [35,36].

We made a series of gravimetric measurements to assess the total aerosolized lipid deposition as well as its deposition versus time when using the vibrating mesh nebulizer. A thin piece of aluminum foil was weighed and placed over the portion of an unfilled trough within the enclosure to mimic the area and location of aerosol deposition in the experiment. The nebulizer was then allowed to deliver a known volume of DMPC dispersion. The foil was dried in a vacuum oven overnight and then re-weighed to determine the total amount of deposited lipid.

In order to determine the concentration of the nebulizer output with time, we aerosolized lipid for multiple consecutive two-minute periods directly into a series of pre-weighed beakers. We then weighed each liquid-filled beaker, dried each in a vacuum oven overnight, and then re-weighed the dry lipid. The results, shown in Fig. 2, indicate the concentration of the lipid in the aerosol increases as the nebulizer reservoir empties.

We used ellipsometry to characterize the phospholipid layer deposited from the aerosol onto the water surface. Because the experimental trough was too narrow to align under the ellipsometer, measurements were performed on a half-covered 14 cm petri dish with direct deposition in the uncovered region and transport into the covered region. Ellipsometric results were the same both within and outside the region of deposition. The surface layer was probed using the 632.8 nm laser beam of a phase-modulation picometer ellipsometer (Beaglehole Instruments,

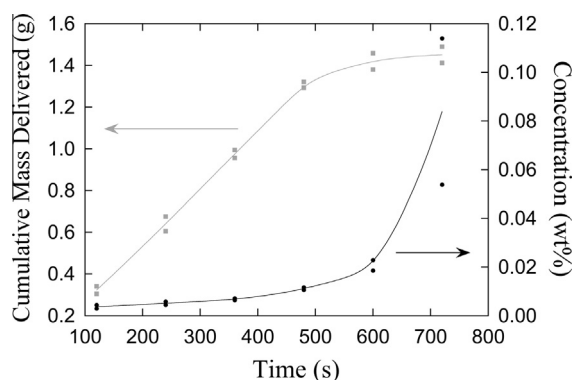


**Fig. 2.** Cumulative liquid mass delivered by the nebulizer and lipid concentration in the DMPC aerosol taken simultaneously (data for two trials plotted). Error bars on experimental mass measurement are  $\pm 0.0001$  g, which is within plotted points. These are measurements made over two minute intervals, which average over unsteady output of the nebulizer. The lines are guides to the eye.

Ltd.). Measurements were made near the Brewster angle, 52°, at three spatially separated points on the surface to check for consistency. The standard ellipsometric parameter  $\Delta$  was reported for DMPC monolayers deposited out of chloroform and compared with the  $\Delta$  values for a layer created via aerosolization.

To analyze the fate of all material being delivered in addition to the monolayer at the surface, we also monitored the sub-surface fluid using dark field microscopy. We used a Nikon AZ100 microscope (Nikon Instruments Inc, Melville, NY) with an AZ-Plan Apo 4 × objective and 8 × zoom. The microscope camera (model DS-QiMc-Nikon) had 0.6 × magnification. This allowed us to detect and track lipid aggregates that appeared in the subphase during aerosol deposition.

### 3. Results and discussion

#### 3.1. Deposition of microliter drops and aerosolized dispersion

As shown in Fig. 3A, microliter drops of DMPC MLV dispersion neither reduce the surface tension outside the drop nor induce Marangoni flow. This figure depicts a typical trial in which a series

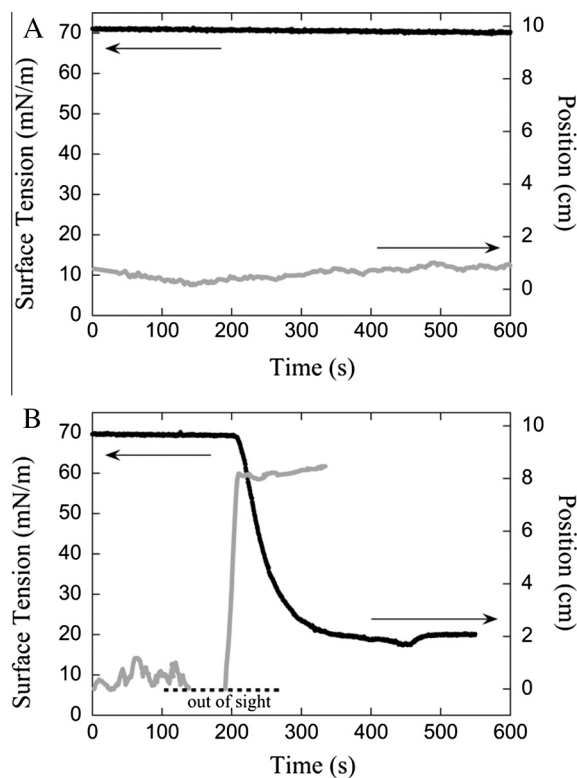


**Fig. 3.** Simultaneous measurements of surface tension and indicator bead position for two modes of lipid dispersion deposition. (A) Deposition of microliter drops of 10 mg/mL DMPC dispersion onto a DI water subphase. Ten  $\mu\text{L}$  droplets of 10 mg/mL DMPC were deposited every 10 s for the duration of the experiment. (B) A representative plot of surface tension and position versus time during aerosolized DMPC dispersion deposition. In this trial, 4 mL of 10 mg/mL DMPC dispersion were aerosolized via an AeroNeb Solo vibrating mesh nebulizer onto a clean DI water surface. Aerosol deposition begins at 0 s and ends at 450 s. The Wilhelmy pin is located at approximately 9 cm.

of 10  $\mu\text{L}$  drops of 10 mg/mL DMPC dispersion were pipetted onto a clean water surface every 10 s. Upon deposition of these drops, a very small decrease in surface tension from that of water is discernable, with a fitted slope of  $\sim 0.001$  mN/m/s, and the indicator particle on the surface does not move beyond observed baseline average noise arising from extrinsic laboratory conditions including minor vibrations and air currents. During this experiment, enough total lipid monomer was deposited to create over 600 lipid monolayers on the trough surface, yet there was still no indication of surface tension reduction or indicator bead transport. These results show that drops of DMPC MLV dispersion do not contain enough available surface-active material to create a surface tension gradient sufficient to induce Marangoni flow or to lower the surface tension remote from the deposition location. Similar negative results were seen with drop-wise deposition of fluid-phase SUV dispersions that had been prepared by ultrasonication.

In order to determine if the mere process of nebulization would be sufficient to create dispersions capable of inducing Marangoni flow, we also deposited microliter drops of freshly nebulized dispersion with very similar negative results. In these experiments, a 10 mg/mL DMPC dispersion was nebulized directly into a beaker and then 10  $\mu\text{L}$  drops of this freshly collected aerosolized dispersion, taken from the bulk fluid below the surface, were successively pipetted onto a clean water surface. The drops were pipetted within a minute of being aerosolized, yet they also showed no ability to lower the surface tension of the water remote from the point of drop deposition or to move an indicator particle. Since we will show in the next paragraph that the direct aerosolization process

does deliver surface-active species to the subphase surface, the negative result here must be due to re-aggregation of the surface-active species within a minute of the aerosol droplets being subsumed into a bulk fluid in the beaker. These results are similar to those of Minocchieri and coworkers, who report cryo-TEM evidence that nebulized Curosurf SRT vesicles re-aggregate rapidly after nebulization into bulk fluid [23].

As shown in Fig. 3B, aerosolized lipid dispersions deposited directly from the aerosol phase onto the subphase surface do reduce surface tension outside of the deposition region and do induce Marangoni flow. Four mL of 10 mg/mL DMPC dispersion were aerosolized via an AeroNeb vibrating mesh nebulizer above a clean DI water surface while the surface tension and bead position were monitored as a function of time outside the region of direct deposition. For the experiment shown in Fig. 3B, the nebulizer is turned on at 0 s. For the first 2 min of deposition, the surface tension decreases very slowly, at a rate of approximately 0.002 mN/m/s. During this time, the bead position fluctuates on the surface with a standard deviation in position of 0.3 cm, likely due to air currents and vibrations, but its average location does not change significantly. In the case shown, at approximately 2 min, the bead's fluctuations on the surface carry it into the containment box, out of the field of view of the camera. At approximately 3 min, the Marangoni flow overcomes the random motions of the bead, and it begins to move across the surface at a velocity of  $\sim 0.37$  cm/s; the average speed over seven such trials is  $0.20 \pm 0.1$  cm/s with the variation dominated by run-to-run differences. Here we chose to show an experiment with a slightly above-average transport speed due to the clarity with which this experiment showed all common aspects of these trials. The bead completely traverses the trough within 30 s of the initiation of consistent motion. This motion across the surface is coincident with a lowering of the subphase surface tension. The bead's motion is stopped only when it reaches the end of the trough and runs into the meniscus on the Wilhelmy pin. Control experiments performed either without the pin or without the indicator bead show that the surface tension reduction and bead motion occur independently, ruling out any mechanically significant contributions from pin-bead interactions.

In all experiments, aerosolized DMPC deposition resulted in a surface tension reduction to values below  $18 \pm 4$  mN/m. When aerosol was deposited continuously and was not limited by exhaustion of the reservoir dose, surface tensions as low as 1 mN/m could be achieved, as will be discussed below.

There is typically a 3–6 min delay between the start of aerosolization and the convective movement of the bead across the surface. The Marangoni stress across the trough is initially quite small, resulting in a surface flow that is too weak to overcome the noise-level movements of the bead. There are at least two reasons why the gradient is small at early times. First, the nebulizer delivers an initially low concentration of lipid to the surface as shown in Fig. 2. Second, the monolayer isotherm shows that the lipid surface concentration must build to between 130 and 90  $\text{\AA}^2$ /molecule before the monolayer leaves the gaseous phase and develops a significant surface pressure.

### 3.2. Structure and dynamics of surface lipid layer

We used ellipsometry to probe the structure of the surface lipid layer created through aerosol deposition. As a baseline for comparison, a DMPC monolayer was created by sequential deposition of drops of lipid dissolved in chloroform. The chloroform was allowed to evaporate, and then the change in the ellipsometric parameter  $\Delta$  from the bare subphase was measured. According to the surface pressure/area isotherm (Supporting Information Fig. S2) above approximately 0.015 molecules per  $\text{\AA}^2$ , the monolayer begins to

collapse, which means the molecule per area values no longer represent molecular packing in a monolayer. The change in  $\Delta$  from the resulting monolayer plateaus at  $5.1 \pm 0.1^\circ$ . Ellipsometry was then performed on the lipid layer formed outside of the region of direct DMPC aerosol deposition in a half-covered petri dish. This experiment was done in a stepwise manner by nebulizing for a minute, turning off the nebulizer and taking a measurement, and repeating until the nebulizer was empty. To check that the stopping and starting of the nebulizer had no effect on the layer thickness, this experiment was then repeated without stopping the nebulizer and only the final ellipsometric thickness was taken. The aerosolized DMPC layer thickness plateaus at an ellipsometric parameter  $\Delta$  of  $5.5 \pm 0.4^\circ$ . This strongly suggests that aerosolization causes a monolayer of DMPC to move out of the region of aerosol deposition and across the subphase surface (see Fig. 4).

Since the ellipsometric data indicate that a monolayer of lipid is forming outside the direct deposition region, we may use our surface pressure/area isotherm to determine the surface density of the lipid in the monolayer on the water surface. For the data in Fig. 3, the surface tension at 280 s, 27 mN/m, indicates a surface density of 1.7 molecules/nm<sup>2</sup> according to the surface pressure/area isotherm in Supplemental Information Fig. S2, and thus a total of  $6.9 \times 10^{15}$  molecules or 7.8  $\mu\text{g}$ , in the monolayer on the trough. However, when we weigh the total amount of dry lipid delivered to the surface in a full trial, we get an average total mass of  $5.5 \pm 0.2$  mg. Adjusting for the fact that these full trial drying experiments run longer than the 280 s in the above figure, we can estimate that lipid quantities on the order of a milligram have been delivered by the time in question. Clearly, a significant amount of the total lipid delivered to the trough is not contained in the monolayer.

Using dark field microscopy, we were able to visualize the remaining non-monomeric lipid deposited from the aerosol. As shown in Fig. 5, in the region of direct aerosol deposition immediately post-deposition, we see  $\sim 10$   $\mu\text{m}$  static bright spots that permeate a layer from just below the surface to a depth of  $\sim 0.5$  mm in the water. These bright spots are not present in a control where pure water is aerosolized, leading to the conclusion that the bright spots are lipid aggregates.

These aggregates have unknown structure and are therefore described as “clusters”. As shown in Fig. 6, in a region outside of the area of direct deposition and just below the surface, we observe that these clusters are transported beneath the surface by the

induced Marangoni flow. They travel outward from the area of deposition in the same manner as the indicator bead does at the surface. The bright spots that are in focus are on the order of 10  $\mu\text{m}$ . These bright spots are so close to the size of individual aerosol drops that they most likely result from the deposition of single droplets (where droplet volume-weighted median diameter is  $5.7 \pm 0.1$   $\mu\text{m}$ ).

We note that clusters of lipid can be seen moving beneath the surface soon after the onset of aerosol deposition and typically on the order of a minute before the onset of indicator bead motion. During this interval, subsurface fluid velocity is seen to increase to a value of  $\sim 0.05$  cm/s found by tracking the position of clusters in consecutive video frames. As expected for subsurface flow, this is slightly smaller than the  $\sim 0.2$  cm/s surface bead velocities described above. The delay in onset of surface bead motion relative to the subsurface flow suggests that the indicator beads ( $\sim 1$  mm) are more susceptible to random extrinsic motion from air currents in the room than the small subsurface clusters ( $\sim 10$   $\mu\text{m}$ ) and, thus, require a stronger Marangoni stress to be driven across the surface.

The combination of these sub-surface images and our ellipsometric data gives a more complete picture of the system. In Fig. 7, we show a schematic of what we believe is happening during aerosolized lipid delivery. Ellipsometry indicates a lipid monolayer at the air-water interface, while sub-surface images indicate that the remainder of lipid resides in aggregates beneath the surface. The monomeric lipid causes local surface tension reduction and a gradient in surface tension across the surface. Any infinitesimal gradient in surface tension across the surface will induce a Marangoni flow across the surface, but the gradient must build sufficiently to overcome the extrinsic fluctuations of the indicator particle.

### 3.3. Observations on other systems

We conducted these transport experiments with two different phospholipids (DMPC and DPPC), at two different initial concentrations in the nebulizer (10 mg/mL and 1 mg/mL), with two different nebulizers (jet and vibrating mesh), and on three different subphases (DI water at 72 mN/m, PA at  $70.8 \pm 0.5$  mN/m, and PGM at  $38.3 \pm 3.5$  mN/m). The results are qualitatively the same in all cases. All experiments showed significant surface tension reduction and transport of the marker particle across the full length of the trough. See supplemental information Fig. S1 for examples.

If either the vibrating mesh or jet nebulizer is reloaded multiple times to produce a continuous supply of lipid to dose the surface, rather than delivering a single-reservoir dose, surface tensions as low as 1 mN/m can be achieved. Such low surface tensions have occasionally been measured on Langmuir troughs for pure phospholipids at an air-water interface. For example, Lee's work shows DPPC monolayer surface tensions close to 0 mN/m when monolayers are compressed to their tightest possible packing [35]. We made visual observations of the meniscus height on the Wilhelmy pin in order to be sure that a changing contact angle was not erroneously causing the pin to report a low surface tension. Although the exact contact angle on the pin was not measured, the meniscus was visible and never significantly decreased in height from pre to post lipid deposition during all experiments, including those at low surface tension. Furthermore, to get a sense of the change in contact angle needed for the pin to read 1 mN/m while the actual surface tension was higher, say 10 mN/m, we analyzed the force balance on the pin. In this case, the contact angle would have had to be  $84^\circ$ , a nearly flat meniscus. The observed meniscus was much more curved than this.

In Fig. 8, we see that both aerosolized DMPC and DPPC dispersions are able to reach these low surface tensions when deposited onto water. This is true for both the vibrating mesh and the jet

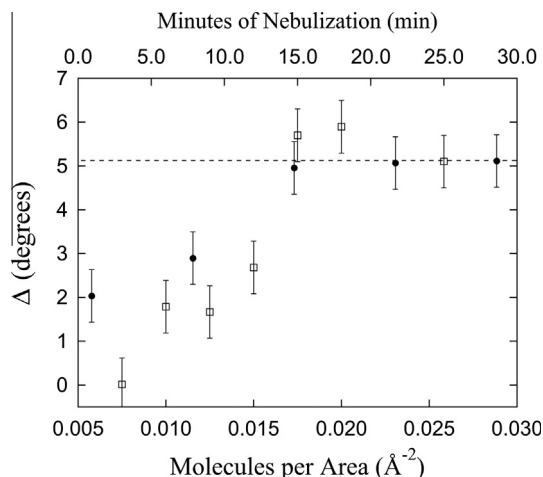
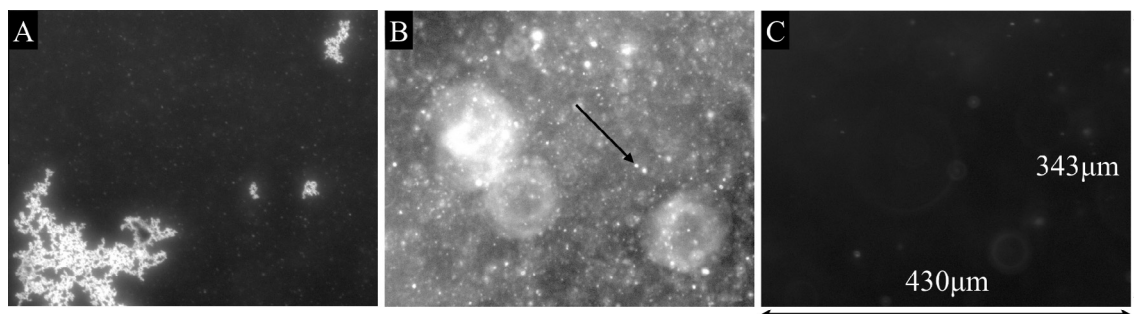
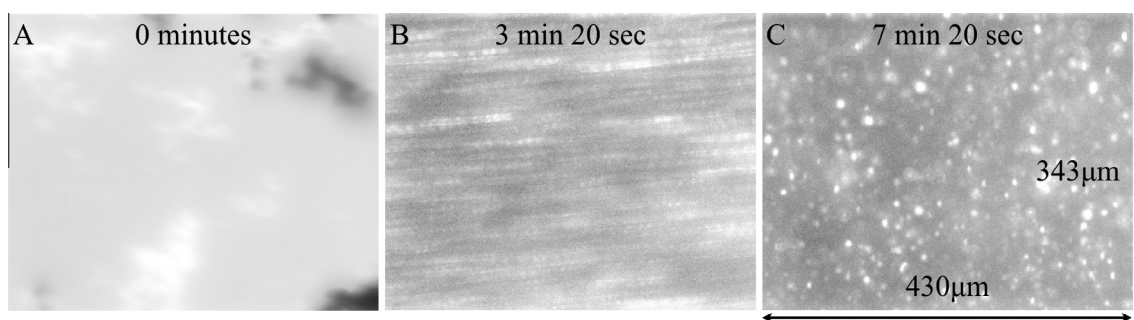


Fig. 4. Ellipsometric parameters of a monolayer deposited out of chloroform (units of molecules per area) shown as filled circles, and a surface layer deposited via aerosolization (units of minutes) shown as open squares. The dashed line marks the saturation of the chloroform-deposited monolayer.



**Fig. 5.** Dark field microscopy images of lipid clusters beneath the surface in the area of aerosol deposition. All panels are 430 by 343  $\mu\text{m}$ . (A) is focused on small chromium dioxide needles that were placed on the water surface in order to be able to focus at the air-liquid interface. (B) is focused  $\sim 60 \mu\text{m}$  beneath the surface. The small ( $\sim 10 \mu\text{m}$ ), sharply focused bright spots are clusters of lipid. The arrow in panel B points to one such small cluster. The larger, less focused features are the out-of-focus chromium dioxide needles on the surface or other out-of-focus lipid clusters. (C) is focused  $\sim 420 \mu\text{m}$  below the surface and shows very few lipid clusters have been transported this deep into the subphase.



**Fig. 6.** Dark field microscopy images of lipid cluster transport outside of the area of deposition. All panels are 430 by 343  $\mu\text{m}$  and focused  $\sim 60 \mu\text{m}$  beneath the surface. (A) shows out-of-focus chromium dioxide needles before the nebulizer is turned on. (B) occurs during deposition and shows lipid clusters moving across the field of view beneath the surface at  $\sim 0.05 \text{ cm/s}$ . By 7 min: 20 s, shown in (C), subsurface lipid clusters are still evident, but lateral flow has ceased.

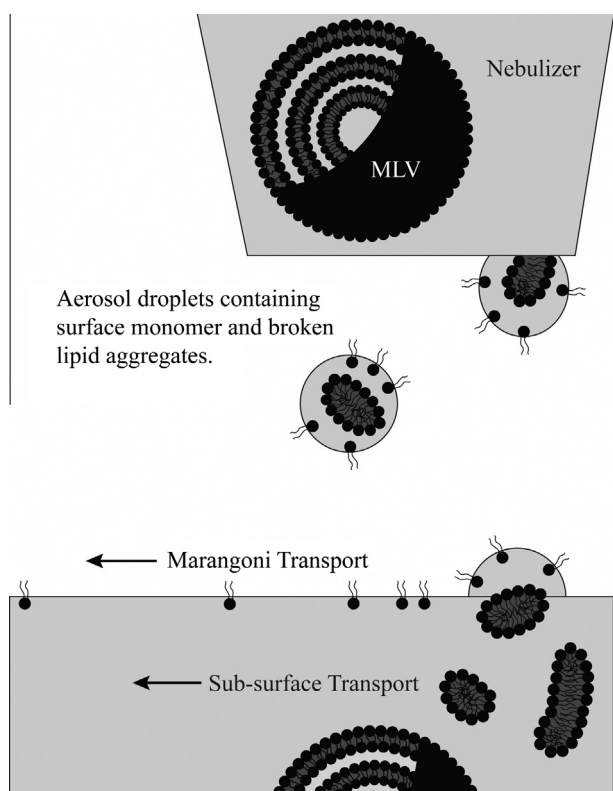


**Fig. 7.** Schematic of how aerosolization disrupts vesicles, stores monomeric lipid as an adsorbed layer on droplets, delivers monomeric lipid to the subphase surface and vesicle fragments to the subphase bulk, releases monomeric lipids, and transports clusters.

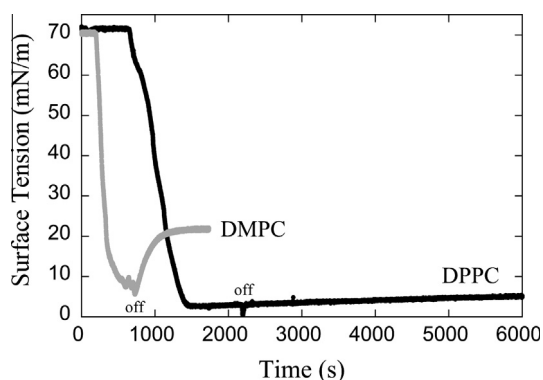


**Fig. 8.** Representative low surface tension results for DPPC and DMPC dispersion aerosols deposited on DI water. Both lipids are able to reach very low surface tensions ( $<10 \text{ mN/m}$ ). In these trials, the vibrating mesh nebulizer was turned on at 60 s and turned off at the label “off”. The DPPC monolayer is relatively stable after the nebulizer is turned off, while the DMPC monolayer destabilizes and the surface tension increases to  $\sim 20 \text{ mN/m}$ .

nebulizers as long as the dispersion supply in the reservoir is sufficiently large. The one clear difference between these experiments is the fact that the DPPC layer remains at a low surface tension, increasing slowly after the end of aerosolization, but remaining below  $10 \text{ mN/m}$  even when left overnight. DMPC, on the other hand, recovers to about  $20 \text{ mN/m}$  within a few minutes after aerosolization is stopped. At the temperature of these experiments, DMPC will be in a fluid phase while DPPC will be in a gel phase. According to the work of Lee and coworkers, DPPC's greater rigidity at a temperature below its gel transition allows it to sustain much lower surface tensions than it could above the transition

temperature [35,37–39]. DMPC's more fluid phase in the current experiments conducted slightly above its gel transition would not allow it to sustain such low surface tensions. Collapse pressures for lipid monolayers depend heavily on temperature.

However, the temperature dependence of the collapse pressure does not explain why the DMPC layers dip to very low surface tensions but then recover. Langmuir trough studies suggest there is a competition between the rate at which lipid is being compressed on the surface and the rate at which material is being lost to the subphase [35]. By continually feeding the monolayer with monomeric lipids from the aerosol, we are compressing it outside the region of direct aerosol deposition where the surface tension is measured. As it is being continuously fed, we hypothesize that the DMPC monolayer may be able to sustain a higher surface pressure state than it generally would at this temperature.

#### 4. Conclusions

We have shown that when lipid dispersions are aerosolized onto an air-aqueous interface, they can produce Marangoni flow, whereas macroscopic droplets of the same dispersions cannot produce this flow. Lipid dispersions do not contain enough accessible surface-active material to initiate detectable Marangoni flow because the lipid is sequestered within non-surface-active vesicles. We propose that aerosolization acts both to shear open vesicles and to create a high droplet surface area on which to store monomeric lipid until it is deposited and transferred onto the subphase surface. Aerosolization of the lipid dispersion and direct deposition of the resulting aerosol are both required for significant Marangoni flow. If the aerosol drops are allowed to recombine in a bulk medium before deposition, the broken lipid structures quickly re-aggregate, leaving a bulk dispersion incapable of producing Marangoni stresses.

When the aerosol droplets land on the subphase, they transfer stored monomeric lipid directly onto the surface. They also deliver the non-surface-active aggregate fragments to the bulk. Being non-surface-active, these aggregates diffuse from the surface region deeper into the (initially lipid-free) bulk, appearing within a thin region on the order of hundreds of micrometers from the surface on the time scale of these experiments. In contrast with what has been shown for bulk dispersions, these clusters evidently are not adsorbed onto or otherwise associated with the lipid monolayer. If there were aggregates attached to the surface, as Kim and coworkers observed in their work with bulk dispersions of pure lipid vesicles [14], ellipsometry would have revealed a thicker surface layer rather than the observed monolayer. With increasing deposition, the packing of this monolayer increases until it creates a sufficient surface tension gradient between the deposition region and the remote surface to induce a Marangoni flow strong enough to carry tracer particles. Characteristic of Marangoni flow, the surface flow induces a subsurface flow within the bulk, which causes convection of lipid clusters beneath the surface.

Because surface tension gradients may be maintained down to very low surface tensions with aerosolized lipid deposition, these dispersions are able to induce Marangoni flow on subphases, such as PGM, that have surface tensions lower than the limiting surface tensions of many common soluble surfactants. Use of surfactant-driven Marangoni flows to enhance the distribution of aerosolized medication in pulmonary drug delivery would depend not only on the ability to drive Marangoni flow on complex lung airway surface liquids with variable surface tensions, but also on their safety in the lung. As natural components of the pulmonary surfactant that is abundant in the respiratory zone of the lung, phospholipids are good candidates for enhanced pulmonary drug delivery in the bronchi and bronchioles. This work has shown that phospholipids

can function as Marangoni spreading agents, provided they are administered via aerosol deposition, without the need for any other excipients. The observation that a very small fraction of the overall lipid delivered is capable of driving flow over large distances is a strong indication of the applicability of this method for pulmonary drug delivery.

The ability to induce Marangoni flow on very low surface tension surfaces is essential if we wish to apply this work to therapeutic applications in the lung, either for enhanced drug delivery using self-dispersing aerosolized carriers or for delivery of SRT formulations. Although the surface tension, and its spatial variation, in the lung is not agreed upon in the literature [40–43], the fact that surface tensions as low as 1 mN/m can be achieved using aerosolized lipid dispersions means that there is a good chance that these dispersions will spread well in the lung. In addition, the fact that we consistently observe convection beneath the surface suggests that any drug that one may disperse with (or encapsulate in) lipid vesicles will be transported by convection over large distances after deposition. This would allow the delivery of aerosolized lipid dispersions to aid in transport of non-surface-active medication to the lung.

Our future work will focus on understanding these induced Marangoni flows in more complex systems. The simplified systems used in these experiments do not capture the lung's compound layers of fluid and cells, its pre-existing surfactant content, its cylindrical geometry, or its ability to perform mucociliary clearance. These complexities may alter or limit Marangoni transport. We have already begun to examine the ability of lipid dispersions to cause fluid flow against pre-existing phospholipid monolayers on water. We have also begun to test Marangoni spreading in cylindrical geometries with very thin (100 nm) fluid layers.

#### Acknowledgements

Research reported in this publication was supported by the National Heart, Lung and Blood Institute of the National Institutes of Health under Award Number R01 HL105470. The content is solely the responsibility of the authors and does not necessarily represent the official views of the National Institutes of Health. In addition, we would like to thank Dr. John Riley and Emily Walitsch for their ellipsometry expertise and Joseph Nero for his aid in aerosol sizing.

#### Appendix A. Supplementary material

Supplementary data associated with this article can be found, in the online version, at <http://dx.doi.org/10.1016/j.jcis.2016.08.076>.

#### References

- [1] J.B. Grotberg, D.P. Gaver, A synopsis of surfactant spreading research, *J. Colloid Interface Sci.* 178 (1996) 377–378, <http://dx.doi.org/10.1006/jcis.1996.0130>.
- [2] D.P. Gaver, J.B. Grotberg, Droplet spreading on a thin viscous film, *J. Fluid Mech.* 235 (1992) 399–414, <http://dx.doi.org/10.1017/S0022112092001162>.
- [3] D.P. Gaver, J.B. Grotberg, The dynamics of a localized surfactant on a thin film, *J. Fluid Mech.* (1990), <http://dx.doi.org/10.1017/S0022112090002257>.
- [4] A.B. Afsar-Siddiqui, P.F. Luckham, O.K. Matar, The spreading of surfactant solutions on thin liquid films, *Adv. Colloid Interface Sci.* 106 (2003) 183–236, [http://dx.doi.org/10.1016/S0001-8686\(03\)00111-8](http://dx.doi.org/10.1016/S0001-8686(03)00111-8).
- [5] J.B. Grotberg, Respiratory fluid mechanics and transport processes, *Annu. Rev. Biomed. Eng.* 3 (2001) 421–457, <http://dx.doi.org/10.1146/annurev.bioeng.3.1.421>.
- [6] D. Halpern, O.E. Jensen, J.B. Grotberg, A theoretical study of surfactant and liquid delivery into the lung, *J. Appl. Physiol.* 85 (1998) 333–352.
- [7] C.D. Bertram, D.P. Gaver, Biofluid mechanics of the pulmonary system, *Ann. Biomed. Eng.* 33 (2005) 1681–1688, <http://dx.doi.org/10.1007/s10439-005-8758-0>.
- [8] A. Khanal, R. Sharma, T.E. Corcoran, S. Garoff, T.M. Przybycien, R.D. Tilton, Surfactant driven post-deposition spreading of aerosols on complex aqueous subphases. 1: High deposition flux representative of aerosol delivery to large

- airways, *J. Aerosol Med. Pulm. Drug Delivery* 28 (2015) 382–393, <http://dx.doi.org/10.1089/jamp.2014.1168>.
- [9] R. Sharma, A. Khanal, T.E. Corcoran, S. Garoff, T.M. Przybycien, R.D. Tilton, Surfactant driven post-deposition spreading of aerosols on complex aqueous subphases. 2: Low deposition flux representative of aerosol delivery to small airways, *J. Aerosol Med. Pulmonary, Drug Delivery* 28 (2015) 394–405, <http://dx.doi.org/10.1089/jamp.2014.1167>.
- [10] R. Sharma, T.E. Corcoran, S. Garoff, T.M. Przybycien, E.R. Swanson, R.D. Tilton, Quasi-immiscible spreading of aqueous surfactant solutions on entangled aqueous polymer solution subphases, *ACS Appl. Mater. Interfaces* 5 (2013) 5542–5549, <http://dx.doi.org/10.1021/am400762q>.
- [11] K. Koch, B. Dew, T.E. Corcoran, T.M. Przybycien, R.D. Tilton, S. Garoff, Surface tension gradient driven spreading on aqueous mucin solutions: a possible route to enhanced pulmonary drug delivery, *Mol. Pharm.* 8 (2011) 387–394, <http://dx.doi.org/10.1021/mp1002448>.
- [12] A.L. Marcinkowski, S. Garoff, R.D. Tilton, J.M. Pilewski, T.E. Corcoran, Postdeposition dispersion of aerosol medications using surfactant carriers, *J. Aerosol Med. Pulmonary Drug Delivery* 21 (2008) 361–370, <http://dx.doi.org/10.1089/jamp.2008.0699>.
- [13] S.H. Kim, E.I. Franses, New protocols for preparing dipalmitoylphosphatidylcholine dispersions and controlling surface tension and competitive adsorption with albumin at the air/aqueous interface, *Colloids Surf., B* 43 (2005) 256–266, <http://dx.doi.org/10.1016/j.colsurfb.2005.05.006>.
- [14] S.H. Kim, Y. Park, S. Matalon, E.I. Franses, Effect of buffer composition and preparation protocol on the dispersion stability and interfacial behavior of aqueous DPPC dispersions, *Colloids Surf., B* 67 (2008) 253–260, <http://dx.doi.org/10.1016/j.colsurfb.2008.09.003>.
- [15] S.H. Kim, L. Haimovich-Caspi, L. Omer, Y. Talmon, E.I. Franses, Effect of sonication and freezing–thawing on the aggregate size and dynamic surface tension of aqueous DPPC dispersions, *J. Colloid Interface Sci.* 311 (2007) 217–227, <http://dx.doi.org/10.1016/j.jcis.2007.02.060>.
- [16] M.A. Launois-Surpas, T. Ivanova, I. Panaiotov, Behavior of pure and mixed DPPC liposomes spread or adsorbed at the air–water interface, *Colloid Polym. Sci.* (1992), <http://dx.doi.org/10.1007/BF00657735>.
- [17] J. Ding, D.Y. Takamoto, A. von Nahmen, M.M. Lipp, K.Y.C. Lee, A.J. Waring, J.A. Zasadzinski, Effects of lung surfactant proteins, SP-B and SP-C, and palmitic acid on monolayer stability, *Biophys. J.* 80 (2001) 2262–2272, [http://dx.doi.org/10.1016/S0006-3495\(01\)76198-X](http://dx.doi.org/10.1016/S0006-3495(01)76198-X).
- [18] M.M. Lipp, K.Y.C. Lee, J.A. Zasadzinski, A.J. Waring, Design and performance of an integrated fluorescence, polarized fluorescence, and Brewster angle microscope/Langmuir trough assembly for the study of lung surfactant monolayers, *Rev. Sci. Instrum.* 68 (1997) 2574–2582, <http://dx.doi.org/10.1063/1.1148163>.
- [19] X. Wen, E.I. Franses, Role of subsurface particulates on the dynamic adsorption of dipalmitoylphosphatidylcholine at the air/water interface, *Langmuir* 17 (2001) 3194–3201, <http://dx.doi.org/10.1021/la001502t>.
- [20] J.T. Buboltz, G.W. Feigenson, Phospholipid solubility determined by equilibrium distribution between surface and bulk phases, *Langmuir* 21 (2005) 6296–6301, <http://dx.doi.org/10.1021/la047086k>.
- [21] B.E. Gilbert, H.R. Six, S.Z. Wilson, P.R. Wyde, V. Knight, Small particle aerosols of enviroxime-containing liposomes, *Antivir. Res.* 9 (1988) 355–365.
- [22] K.M.G. Taylor, G. Taylor, I.W. Kellaway, J. Stevens, The stability of liposomes to nebulisation, *Int. J. Pharm.* 58 (1990) 57–61.
- [23] S. Minocchieri, S. Knoch, W.M. Schoel, M. Ochs, M. Nelle, Nebulizing poractant alfa versus conventional instillation: ultrastructural appearance and preservation of surface activity, *Pediatr. Pulmonol.* 49 (2014) 348–356, <http://dx.doi.org/10.1002/ppul.22838>.
- [24] M. Caffrey, J. Hogan, LIPIDAT: a database of lipid phase transition temperatures and enthalpy changes. DMPC data subset analysis, *Chem. Phys. Lipids* 61 (1992) 1–109.
- [25] M.C. Wiener, S. Tristram-Nagle, D.A. Wilkinson, L.E. Campbell, J.F. Nagle, Specific volumes of lipids in fully hydrated bilayer dispersions, *Biochim. Biophys. Acta* 938 (1988) 135–142.
- [26] S. Tristram-Nagle, M.C. Wiener, C.P. Yang, J.F. Nagle, Kinetics of the subtransition in dipalmitoylphosphatidylcholine, *Biochemistry* 26 (1987) 4288–4294.
- [27] S.M. Gruner, R.P. Lenk, A.S. Janoff, M.J. Ostro, Novel multilayered lipid vesicles - comparison of physical characteristics of multilamellar liposomes and stable plurilamellar vesicles, *Biochemistry* 24 (1985) 2833–2842, <http://dx.doi.org/10.1021/bi00333a004>.
- [28] E. Reimhult, F. Hook, B. Kasemo, Intact vesicle adsorption and supported biomembrane formation from vesicles in solution: influence of surface chemistry, vesicle size, temperature, and osmotic pressure, *Langmuir* 19 (2003) 1681–1691, <http://dx.doi.org/10.1021/la0263920>.
- [29] F.L. Grohmann, F. Csempez, M. Szogyi, Stabilization of small unilamellar DMPC-liposomes by uncharged polymers, *Colloid Polym. Sci.* 276 (1998) 66–71, <http://dx.doi.org/10.1007/s003960050210>.
- [30] R. Bansil, H.E. Stanley, J.T. Lamont, Mucin biophysics, *Annu. Rev. Physiol.* 57 (1995) 635–657, <http://dx.doi.org/10.1146/annurev.ph.57.030195.003223>.
- [31] M. Gudmand, M. Fidorra, T. Bjöslashrholm, T. Heimburg, Diffusion and partitioning of fluorescent lipid probes in phospholipid monolayers, *Biophys. J.* 96 (2009) 4598–4609, <http://dx.doi.org/10.1016/j.bpj.2009.01.063>.
- [32] F. Gaboriaud, R. Golan, R. Volinsky, A. Berman, R. Jelinek, Organization and structural properties of langmuir films composed of conjugated polydiacetylene and phospholipids, *Langmuir* 17 (2001) 3651–3657, <http://dx.doi.org/10.1021/la0012790>.
- [33] F. Gaboriaud, R. Volinsky, A. Berman, R. Jelinek, Temperature dependence of the organization and molecular interactions within phospholipid/diacetylene Langmuir films, *J. Colloid Interface Sci.* 287 (2005) 191–197, <http://dx.doi.org/10.1016/j.jcis.2005.01.110>.
- [34] I. Kubo, S. Adachi, H. Maeda, A. Seki, Phosphatidylcholine monolayers observed with Brewster angle microscopy and  $\pi$ -A isotherms, *Thin Solid Films* 393 (2001) 80–85, [http://dx.doi.org/10.1016/S0040-6090\(01\)01101-4](http://dx.doi.org/10.1016/S0040-6090(01)01101-4).
- [35] K.Y.C. Lee, Collapse mechanisms of Langmuir monolayers, *Annu. Rev. Phys. Chem.* 59 (2008) 771–791, <http://dx.doi.org/10.1146/annurev.physchem.58.032806.104619>.
- [36] S.L. Duncan, R.G. Larson, Comparing experimental and simulated pressure-area isotherms for DPPC, *Biophys. J.* 94 (2008) 2965–2986, <http://dx.doi.org/10.1529/biophysj.107.114215>.
- [37] A. Gopal, K.Y.C. Lee, Headgroup percolation and collapse of condensed langmuir monolayers, *J. Phys. Chem. B* 110 (2006) 22079–22087, <http://dx.doi.org/10.1021/jp061562t>.
- [38] A. Gopal, K.Y.C. Lee, Morphology and collapse transitions in binary phospholipid monolayers, *J. Phys. Chem. B* 105 (2001) 10348–10354, <http://dx.doi.org/10.1021/jp012532n>.
- [39] L. Pocivavsek, S.L. Frey, K. Krishan, K. Gavrillov, P. Ruchala, A.J. Waring, et al., Lateral stress relaxation and collapse in lipid monolayers, *Soft Matter* 4 (2008) 2019–2029, <http://dx.doi.org/10.1039/b804611e>.
- [40] S. Schürch, J. Goerke, J.A. Clements, Direct determination of surface tension in the lung, *Proc. Natl. Acad. Sci. U.S.A.* 73 (1976) 4698–4702.
- [41] B.A. Hills, Alveolar liquid lining - langmuir method used to measure surface-tension in bovine and canine lung extracts, *J. Physiol. (Lond.)* 359 (1985) 65–79.
- [42] G.M. Albers, R.P. Tomkiewicz, M.K. May, O.E. Ramirez, B.K. Rubin, Ring distraction technique for measuring surface tension of sputum: relationship to sputum clearability, *J. Appl. Physiol.* 81 (1996) 2690–2695.
- [43] S.M.I. Saad, Z. Policova, E.J. Acosta, A.W. Neumann, Effect of surfactant concentration, compression ratio and compression rate on the surface activity and dynamic properties of a lung surfactant, *BBA - Biomembranes* 1818 (2012) 103–116, <http://dx.doi.org/10.1016/j.bbamem.2011.10.004>.